Thermodynamic analysis of steam reforming and oxidative steam reforming of propane and butane for hydrogen production

Cui, Xiaoti; Kær, Søren Knudsen

Published in:
International Journal of Hydrogen Energy

DOI (link to publication from Publisher):
10.1016/j.ijhydene.2018.05.083

Publication date:
2018

Document Version
Accepted author manuscript, peer reviewed version

Thermodynamic analysis of steam reforming and oxidative steam reforming of propane and butane for hydrogen production

Xiaoti Cui*, Søren Knudsen Kær

Department of Energy Technology, Aalborg University, Pontoppidanstr. 111, 9220 Aalborg, Denmark

Abstract

Thermodynamic analyses of cracking, partial oxidation (POX), steam reforming (SR) and oxidative steam reforming (OSR) of butane and propane (for comparison) were performed using the Gibbs free energy minimization method under the reaction conditions of T = 250–1000°C, steam-to-carbon ratio (S/C) of 0.5–5 and O_2/HC (hydrocarbon) ratio of 0–2.4. The simulations for the cracking and POX processes showed that olefins and acetylene can be easily generated through the cracking reactions and can be removed by adding an appropriate amount of oxygen. For SR and OSR of propane and butane, predicted carbon formation only occurred at low S/C ratios (< 2) with the maximum level of carbon formation at 550–650°C. For the thermal-neutral conditions, the TN temperatures decrease with the increase of the S/C ratio (except for O/C = 0.6) and the decrease of the O/C ratio. The simulated results for SR or OSR of propane and butane are very close under the investigated conditions.

Keywords:

Thermodynamic analysis; Steam reforming; Oxidative steam reforming; Liquefied petroleum gas; Butane; Carbon formation;

**Corresponding author*
E-mail: *xcu@et.aau.dk*
Phone: *+45 2667 8192*

1. Introduction

Hydrogen or hydrogen-rich gas can be produced by reforming (e.g., steam reforming, oxidative steam forming and dry reforming) and partial oxidation of hydrocarbons or alcohols, e.g., methane, methanol, ethanol, liquefied petroleum gas (LPG), gasoline and diesel [1]. For the distributed production of hydrogen (e.g., on-site steam reformers for refueling stations, portable or domestic uses), LPG is a practical candidate because it takes advantage of a wide distribution network as well as convenient transportation and storage [2]. Propane (C_3H_8) and butane (C_4H_{10}) are the main components in LPG. The volume percentages of propane and butane in LPG vary depending on various standards and climates in different countries, e.g., 92.5% – 100% propane for LPG produced in Canada and 65% – 90% butane for LPG produced in Korea [3].

Experimental studies of the catalytic steam reforming (SR) and partial oxidation (POX) of propane, butane and LPG are available in the literature (propane [4-8], butane [9-11] and LPG [12-17]), focusing on the development of novel catalysts with high stability and activity. Since the steam reforming is an endothermic reaction whereas the partial oxidation is an exothermic reaction, the combination of the two processes known as autothermal reforming (ATR) or oxidative steam reforming (OSR) is usually applied to achieve different goals such as thermal neutrality, control of product composition and suppression of coke formation. Under the SR conditions, coke formation is the main issue both for the nickel and noble metal-based catalysts and can result in the deactivation of the catalysts. Furthermore, steam reforming of the heavier propane and butane is more prone to carbon formation than steam methane reforming (SMR) [18]. Under the OSR conditions, the oxygen in the system can depress coke formation by enhancing the gasification of carbon residues relative to the results obtained in SR conditions [7].

The operating conditions used in the experimental studies are T = 270–1000°C, S/C = 0.06–7, O_2/HC (hydrocarbon) = 0–2.3 and conducted at around the atmospheric pressure. The operating conditions such as the pressure, temperature, steam-to-carbon ratio (S/C), oxygen-to-hydrocarbon ratio (O_2/HC) play important roles in the performance of the catalyst, product composition and energy efficiency of the system [19–21]. Thermodynamic analysis can provide useful and rapid guidance of the proper or optimal zone for these operating conditions, e.g., operating in coke-free zone. Many studies of the thermodynamic analysis of the reforming process of hydrocarbons and alcohols can be found, e.g.,

methane [22–24], natural gas [25], propane [20–21], LPG [26], methanol [27] and butanol [28]. Zeng et al. [20] conducted the thermodynamics analysis on the reaction conditions of OSR of propane using the Gibbs free energy minimization method. The temperature of 700°C, H_2O/C_3H_8 ratio above 7 and O_2/C_3H_8 ratio above 1.3 were proposed in order to obtain a high hydrogen yield, low carbon monoxide yield and avoid coke formation. Wang et al. [21] investigated the reaction conditions of dry reforming (DR) and SR of propane. The temperature range of 925–975 K and H_2O/C_3H_8 ratios of 12–18 were suggested to be favorable conditions for propane steam reforming. Silva et al. [26] compared the thermodynamic analysis results with the experimental data for SR and OSR of LPG with the propane to butane ratio of 1:1. The temperature of 973 K and the H_2O/C_3H_8 ratio of 7 were found to be the most suitable reaction conditions for both SR and OSR of LPG. However, there is still a lack of relevant thermodynamic analysis regarding the SR and OSR of the heavier component butane, which is the main component of LPG in some countries.

In the present study, the thermodynamic analyses of SR and OSR of butane were performed using the Gibbs free energy minimization method. The influences of the reaction conditions such as the temperature, S/C ratio and O_2/HC ratio were investigated and can provide guidance for the operation and design of an LPG steam reformer as well as reformers for heavier fuels (e.g., gasoline and diesel) the decomposition of which could result in the formation of the propane and butane intermediates. SR and OSR of propane were also considered in some results for comparison.

2. Methodology

The method of Gibbs free energy minimization is commonly used for the prediction of the thermodynamic equilibrium composition for a complex reactive system with an initial feed composition, certain phases and temperature and pressure conditions [29]. The process of (oxidative) steam reforming of hydrocarbons includes both the gas phase and the probable solid phase from coke formation. By assuming that the solid phase is a pure solid carbon (graphite) and using the Lagrange multiplier method, the Gibbs free energy minimization for the system can be expressed by the equations considering each species in the gas phase and the total system [22]:

$$\Delta G_{fi}^{\circ g} + RTln\frac{y_i\hat{\varphi}_i P}{p^{\circ}} + \sum_k a_{ik}\lambda_k = 0 \quad (1)$$

$$\sum_{i=1}^{N} n_i \left(\Delta G_{fi}^{\circ g} + RTln\frac{y_i \hat{\varphi}_i P}{p^{\circ}} + \sum_k a_{ik}\lambda_k \right) + n_c \Delta G_{fc(s)}^{\circ} = 0 \quad (2)$$

with the following constraint:

$$\sum_i n_i a_{ik} = A_k \quad (3)$$

where $\Delta G^{\circ g}_{fi}$ is the standard Gibbs free energy of formation of gaseous species i, y_i is the mole fraction of species i, $\hat{\varphi}_i$ is the fugacity coefficient of species i, P and P° are the system pressure and standard state pressure (1 atm), respectively, a_{ik} is the number of the atoms of the k^{th} element present in each molecule of gaseous species i, λ_k is the Lagrange multiplier, and A_k is the total atomic mass of the k^{th} element in the feed. n_i and n_c are the mole number of species i and the solid carbon in the system, respectively, while $\Delta G^{\circ}_{fc(s)}$ is the standard Gibbs free energy of formation of the solid carbon which is assumed to be zero.

The thermodynamic analysis using the Gibbs free energy minimization method was performed using the Aspen Plus V9 (RGibbs reactor) software. The Peng-Robinson model was used as the equation of state. A flow rate of 1 mol/s was set for propane or butane (hereafter referred to n-butane) in the feed. It should be noted that the branched isomer iso-butane was not considered in the feed due to the close Gibbs free energy values of n-butane and iso-butane. The conditions for SR and OSR of butane and propane were considered to be as follows: T = 250–1000°C, S/C = 0.5–5 and O_2/HC = 0–2.4. The main products for SR of butane are H_2, H_2O, CH_4, CO, CO_2 and graphite carbon (O_2 was included in the products for OSR); other possible products such as C_2H_2, C_2H_4, C_2H_6, C_3H_6, C_4H_6, and C_4H_8 were also considered. It should be taken into account that other types of solid carbon can also be generated in the SR or OSR processes. Diaz Alvarado and Gracia [30] analyzed three different carbon representations (graphite, nanotubes and amorphous carbon) for SR of ethanol, and indicated that carbon nanotubes were more favorable at above 400°C. Giehr et al. [24] also presented three carbon products (fullerene C_{60}, graphite and amorphous carbon) for the thermodynamic analysis of dry and steam reforming of methane, and mentioned that graphite was the most stable product among the three investigated carbon types. The present study is limited to the graphite carbon due to its properties are available in the database of Aspen Plus.

The conversion of reactant, selectivity and yield of the product are expressed by the following [6]:

$$C_i = \frac{n_{i,0} - n_{i,e}}{n_{i,0}} \tag{4}$$

$$S_{CO} = \frac{y_{CO,e}}{y_{CO,e} + y_{CO_2,e} + y_{CH_4,e} + y_{carbon,e}} \times 100\%, \quad S_{CO_2} = \frac{y_{CO_2,e}}{y_{CO,e} + y_{CO_2,e} + y_{CH_4,e} + y_{carbon,e}} \times 100\%,$$

$$S_{CH_4} = \frac{y_{CH_4,e}}{y_{CO,e} + y_{CO_2,e} + y_{CH_4,e} + y_{carbon,e}} \times 100\%, \; S_{Carbon} = \frac{y_{Carbon,e}}{y_{CO,e} + y_{CO_2,e} + y_{CH_4,e} + y_{carbon,e}} \times 100\% \tag{5}$$

$$Y_{Carbon,i} = C_i \cdot S_{carbon} \tag{6}$$

where C_i is the conversion for the key reactant *i* (i.e., butane or propane), $n_{i,0}$ is the initial mole number for species *i*, $n_{i,e}$ and $y_{i,e}$ are the mole number and mole fraction (wet basis) for species *i* under the thermodynamic equilibrium state calculated by the Gibbs free energy minimization method respectively, and S_i and $Y_{carbon,\,i}$ represent the selectivity for species *i* and yield of carbon from butane or propane reforming, respectively.

The differences in the conversion and selectivity values between SR or OSR of propane and butane are given by the following:

$$\Delta C_i = C_{i,butane} - C_{i,propane}, \qquad \Delta S_i = S_{i,butane} - S_{i,propane}, \qquad X_i = \frac{S_{i,butane} - S_{i,propane}}{S_{i,butane}} \times 100\% \tag{7}$$

where X_i is a relative value based on the selectivity values obtained by SR or OSR of butane, and is used to evaluate the relative difference between the selectivity values given by SR or OSR of butane and propane.

3 Results and discussions

3.1 Reactions in SR and OSR of butane

The possible reactions in SR and OSR of butane are listed in Table 1 and include the steam reforming, cracking and oxidation of alkanes and olefins in the system, the water gas shift reaction and the carbon formation reactions. It is obvious that the reacting system including butane or LPG is more complex than the steam (or oxidative steam) reforming of methane. For example, olefins can be generated

through catalytic or thermal cracking of the heavier alkanes, and reaction 22 may occur easily and lead to pyrolytic carbon deposition on the surface of the catalyst [18]. It should be noted that the complete steam reforming of the hydrocarbons to carbon dioxide (except butane) and other more complex reactions could occur for this reacting system (e.g., through radical reactions) are not listed in Table 1.

Table 1. Possible reactions in SR and OSR of butane

No.	Reactions	ΔH_{298} (kJ/mol)
	Steam reforming (SR) reactions	
1	$CH_4 + H_2O \leftrightarrow CO + 3H_2$	206
2	$C_2H_4 + 2H_2O \leftrightarrow 2CO + 4H_2$	210
3	$C_2H_6 + 2H_2O \leftrightarrow 2CO + 5H_2$	347
4	$C_3H_6 + 3H_2O \leftrightarrow 3CO + 6H_2$	374
5	$C_3H_8 + 3H_2O \leftrightarrow 3CO + 7H_2$	499
6	$C_4H_6 + 4H_2O \leftrightarrow 4CO + 7H_2$	416[1]
7	$C_4H_8 + 4H_2O \leftrightarrow 4CO + 8H_2$	526[2]
8	$C_4H_{10} + 4H_2O \leftrightarrow 4CO + 9H_2$	651
9	$C_4H_{10} + 8H_2O \leftrightarrow 4CO_2 + 13H_2$	487
	Water gas shift (WGS) reaction	
10	$CO + H_2O \leftrightarrow CO_2 + H_2$	–41
	Cracking and carbon formation reactions	
11	$C_4H_{10} \leftrightarrow C_4H_8 + H_2$	125
12	$C_4H_8 \leftrightarrow C_4H_6 + H_2$	110
13	$C_4H_{10} \leftrightarrow C_3H_6 + CH_4$	72
14	$C_4H_{10} \leftrightarrow C_2H_6 + C_2H_4$	95
15	$C_3H_8 \leftrightarrow C_3H_6 + H_2$	125
16	$C_3H_8 \leftrightarrow C_2H_4 + CH_4$	29
17	$C_2H_6 \leftrightarrow C_2H_4 + H_2$	136
18	$C_2H_4 \leftrightarrow CH_4 + C_{(graphite)}$	–127
19	$CH_4 \leftrightarrow 2H_2 + C_{(graphite)}$	75
20	$2CO \leftrightarrow CO_2 + C_{(graphite)}$	–172
21	$H_2 + CO \leftrightarrow H_2O + C_{(graphite)}$	–131
22	$mC_nH_{2n} \rightarrow (C_nH_{2n})_m \rightarrow$ coke	

	Oxidation reactions	
23	$C_nH_m+0.5nO_2 \rightarrow nCO+0.5mH_2$	
24	$C_nH_m+(n+0.5m)O_2 \rightarrow nCO_2+0.5mH_2O$	
25	$CO + 0.5O_2 \rightarrow CO_2$	–229
26	$C + 0.5O_2 \rightarrow CO$	–111
27	$H_2+0.5O_2 \rightarrow H_2O$	–242

1. C_4H_6 in this reaction represents 1,3-butadiene.

2. C_4H_8 in this reaction represents 1-butene.

3.1.1 Thermodynamic equilibrium constant

The thermodynamic equilibrium constant (*K*) is widely used for the evaluation of the extent of a reaction under different reaction conditions. The *K* values for the main reactions in Table 1 were calculated according to the following [22]:

$$\Delta G_r^\circ = \sum_i \gamma_i \Delta G_{fi}^{\circ g} \tag{8}$$

$$K = exp(\Delta G_r^\circ / RT) \tag{9}$$

where γ_i is the stoichiometric coefficient of species *i* in the reaction, ΔG_r° and $\Delta G_{fi}^{\circ g}$ are the Gibbs free energy change of the reaction and the Gibbs free energy of formation for each species at various temperatures, respectively. The data for $\Delta G_{fi}^{\circ g}$ was provided by the Aspen Properties V9 software.

Since *K* is given by the reaction quotient of the products and reactants in the reaction, a high value of *K* $\gg$ 1 indicates that the reaction occurs in the forward direction, whereas the reverse reaction occurs when *K* $\ll$ 1. Fig. 1 shows the natural logarithm values of the thermodynamic equilibrium constant (*LnK*) for the main reactions plotted versus different temperatures. For the steam reforming reactions 1, 5 and 8 (shown in Table 1), the *LnK* values obviously increase with the increase of the temperature, which means that these endothermic reactions are favorable at high temperatures, e.g., the increased conversion of hydrocarbons with temperature can be found in [6]. The *LnK* value of the water gas shift reaction 10 decreases with the increase of temperature and is close to zero at high temperatures (e.g., –0.5 > *LnK* > 0.5 at *T* > 700°C), indicating that this exothermic reaction is favorable at low temperatures and that the equilibrium can be easily influenced by the composition of the reactants and products in

the reacting system at high temperatures. This result is similar to the results of the analysis for the reverse water gas shift reaction reported in [22].

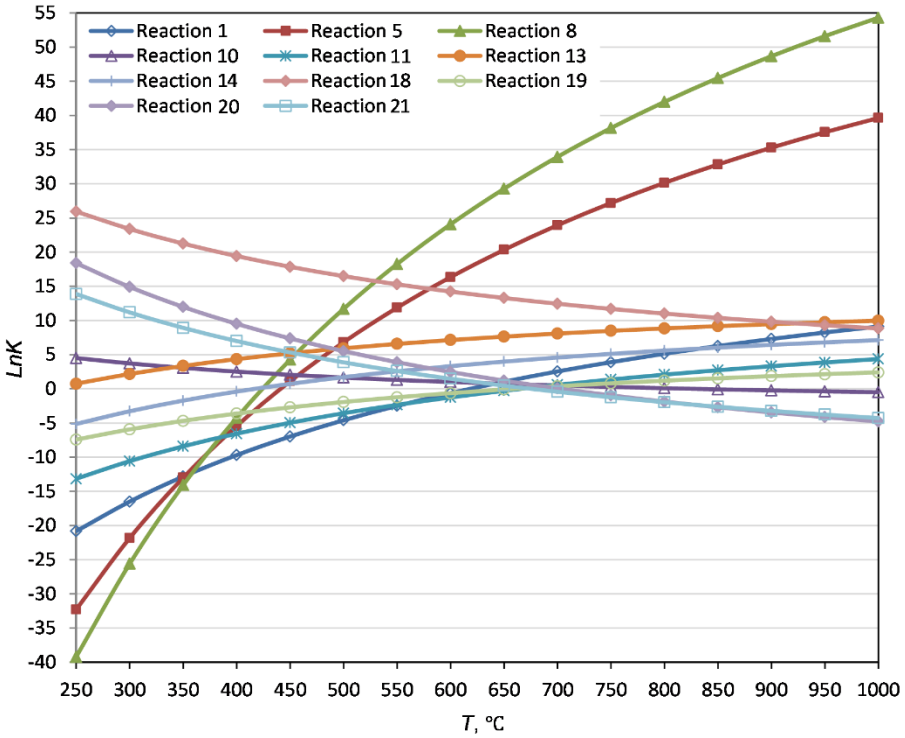

Fig. 1. Equilibrium constants for reactions in SR of butane as a function of temperature at 1 atm.

The *LnK* values of the endothermic cracking reactions of butane 11, 13 and 14 increase with the increase in the temperature. Especially for reaction 13, the positive value of *LnK* indicates that the cracking reaction of the heavy butane is prone to occur at temperatures as low as 250℃. For the carbon formation reactions, the *LnK* value for reaction 18 (cracking of ethylene) has a high value (*LnK* = 11.2–27.3) in the investigated temperature range, indicating that carbon formation from cracking of olefins is also favorable in addition to the carbon deposition via the polymerization reaction 22. The endothermic reaction 19 (decomposition of methane) is the main carbon formation reaction for the SMR process which tends to generate carbon at high temperatures (e.g., *LnK* = 0.38 at T=700℃). Reaction 20 (the Boudouard reaction) and reaction 21 (hydrogenation of carbon monoxide) are exothermic reactions that are favored at low temperature conditions and are limited by high temperature conditions (e.g., *LnK* is below zero at T > 750℃ for reaction 19 and T > 700℃ for reaction 21). The exothermic oxidation

reactions 23–27 occur more easily in the entire temperature range and have high *LnK* values (*LnK* > 16, not shown in Fig. 1).

3.1.2 Cracking and partial oxidation of butane

During the catalytic SR process of butane in a reformer, butane cracking occurs simultaneously on the catalyst (catalytic cracking) and in the gas phase (thermal cracking), which may result in olefins such as ethylene, propylene and acetylene. Since the rate of carbon formation from olefins (through reactions 18 and 22) is much higher than that from alkanes [18], the olefin level in the gas phase of an LPG reformer becomes a critical issue for the carbon formation problem. Therefore, the possible olefin level from the cracking of butane was investigated in this study assuming that no solid carbon was generated in the system.

Fig. 2(a) shows the equilibrium mole flow rates of the products from butane (1 mol/s) cracking at different temperatures (250–1000℃). At low temperatures, cracking occurs with a high conversion of butane, and the amounts of other heavy alkanes (i.e., C_3H_8 and C_2H_6) are found to be small. The main products are methane and the heavy olefins, i.e., 1,3-butadiene and propylene. With the increase of the temperature, further cracking of the heavy alkanes and olefins occurs, resulting in increasing amounts of the light olefin ethylene and acetylene as well as hydrogen. According to the results, at the typical reforming temperature range of 600–900℃, C2–C4 olefins and a small amount of acetylene could exist in the gas phase through the cracking process. Propane cracking was also investigated with similar results shown in Fig. 2(b), and the trends observed at high temperatures (T > 700℃) are consistent with the experimental results for propane steam reforming without catalyst reported in [6], where the olefins (C_2H_4 and C_3H_6) and acetylene were detected in the gas phase.

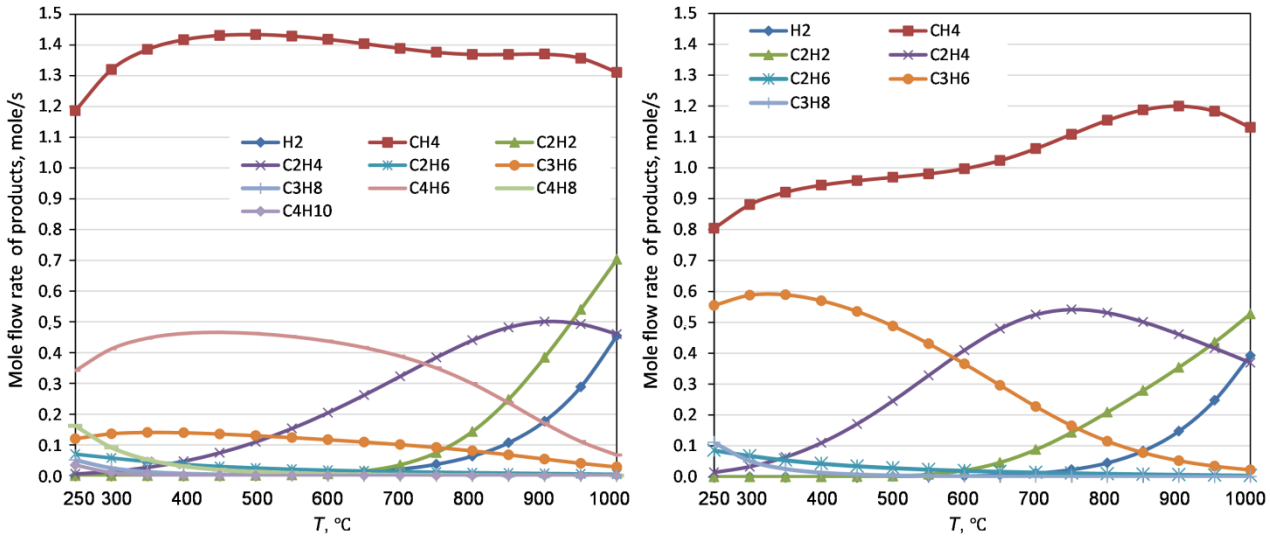

Fig. 2. Mole flow rates of the products for the cracking of (a) butane (1 mol/s) and (b) propane (1 mol/s) as a function of temperature at 1 atm.

For the OSR process of butane, reactions related to the POX of butane (reaction 23–24) are much faster than the steam reforming reactions (reactions 1–9) [31], which could influence the local gas composition (especially the olefin level) and catalyst performance in a reformer with the OSR process. Therefore, an investigation of POX of butane is necessary for the further study of the OSR process of butane. Fig. 3 illustrates the equilibrium mole flow rates of the products from POX of butane (1 mol/s) at different temperatures (250–1000°C) and O_2/C_4H_{10} ratios (O_2/C_4H_{10} = 0.4–1.2, corresponding O/C = 0.2–0.6) in the feed. A complete conversion of oxygen is observed under all the conditions. When a small amount of oxygen (O_2/C_4H_{10} = 0.4) was added in the feed as shown in Fig. 3(a), the trends of the compounds are similar to those of the butane cracking (shown in Fig. 2(a)); however, a fraction of the olefins (C_2H_4, C_3H_6 and C_4H_6) and acetylene in the gas phase were oxidized and generated CO and H_2. The mole flow rates of CO and H_2 are significantly promoted by adding O_2 and increasing temperature, similar trends can be found in the experimental study for the partial oxidation of propane with O_2/C_3H_8 = 1.88 by Silberova and Venvik [4]. When O_2/C_4H_{10} = 0.8 (shown in Fig. 3(b)), the olefins and acetylene in the system were further oxidized and small amounts of C_2H_2 and C_2H_4 are found only at high temperatures (e.g., T > 700°C); this is similar to the experimental result obtained for the homogenous partial oxidation of LPG (O/C = 0.44) as reported by Laosiripojana et al. [14], where

C_2H_4 was also obviously detected in the gas phase at high temperatures (700–900°C). By increasing the O_2/C_4H_{10} ratio to 1.2 as shown in Fig. 3(c), the total level of olefins and acetylene is much lower, e.g., 3–322 ppm with T < 800°C, O_2/C_4H_{10} = 1.2. In additions, the conditions with higher O_2/C_4H_{10} ratios (1.6–2.4) can be found Fig 1S in Appendix A, where only trace amount of olefins were generated in the system.

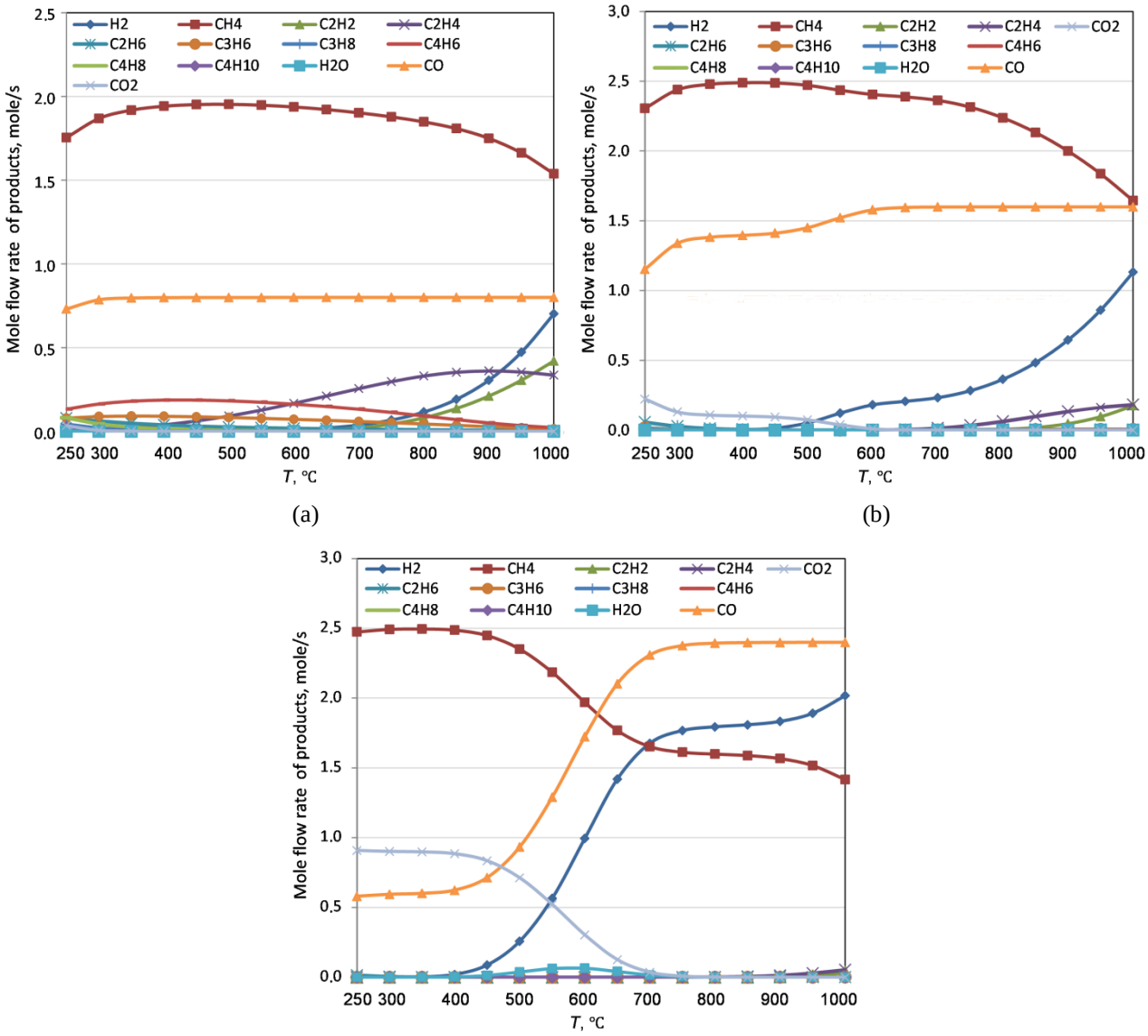

Fig. 3. Mole flow rates of the products of POX of butane (1 mol/s) as a function of temperature and O_2/C_4H_{10} ratio at 1 atm (a) O_2/C_4H_{10} = 0.4; (b) O_2/C_4H_{10} = 0.8; (c) O_2/C_4H_{10} = 1.2.

3.2 Steam reforming of butane

The equilibrium conversion of the reactants, selectivity and yield of the products for SR of butane (1 mol/s) at different temperatures (250–1000℃) and S/C ratios (0.5–5) are shown in Fig. 4. For comparison, the analysis was also performed for propane steam reforming (PSR). The trends from butane steam reforming (BSR) are close to those from PSR both in the present study and in the literature. [21]. Butane was completely converted to CO, CO_2, CH_4 and H_2 under all of the investigated conditions, whereas no olefins and acetylene were found in the product. Solid graphitic carbon was considered in the system.

3.2.1 Conversion of H_2O

Different from the cracking process, steam was added for BSR as a soft oxidant and a source of hydrogen. Steam can also decrease or eliminate the carbon formation on the catalyst surface. A typical S/C ratio for SR of methane is approximately 2.5–3 for industrial-scale hydrogen production [32]. For SR of the heavier propane and butane, a higher S/C ratio could be required because they are more prone to carbon formation than methane [18]. However, a higher S/C ratio can increase the mass flow of steam and relevant investment (e.g., size of reformer) and decrease the conversion of the steam; for example, as shown in Fig. 4(a), for BSR the H_2O conversion decreases with increasing S/C ratio, which is obvious at high temperatures (e.g., T > 600℃). The H_2O conversion for S/C = 1 is close to unity at high temperatures because this ratio fulfils the stoichiometry requirements of the SR reactions (reactions 1–9 for generation of CO and H_2. At low temperatures, the conversions for S/C = 1 and 2 are close, because the WGS reaction (reaction 10) favors low temperature and CO can be further converted to CO_2 by H_2O. Maximum H_2O conversions can be achieved at approximately 600–750 ℃ for S/C = 2–5, and the conversions decrease slightly at higher temperatures. Under the conditions of T > 600℃ and S/C = 2–5, the H_2O conversions are between 30% and 63%. Compared to BSR, the obtained H_2O conversions for PSR (not shown in Fig. 4) are slightly lower with the value differences of ΔC_{H_2O} < 2% for all investigated S/C ratios.

3.2.2 H_2 yield

The H_2 yield in this study was presented as the moles of H_2 produced per mole of butane in the feed, with the obtained results shown in Fig. 4(b). The trend is very similar to that for the propane steam reforming in [21], where H_2 yield increased with the increase of the temperature at low and moderate temperatures and S/C ≥ 2, and then slightly decreased due to the exothermic WGS reaction (reaction 10)

being unfavorable at high temperatures, so that maximum H_2 yields were found at T > 600–750℃. Under the conditions of T > 600℃ and S/C = 2–5, the moles of H_2 produced per mole of butane are between 7.2 and 11.6 mole. Compared to the PSR results, the H_2 amount produced via BSR is 20.9–23.0% higher, because there are two more hydrogen atoms in butane molecule and more water molecules are involved in the SR process for the same S/C ratios.

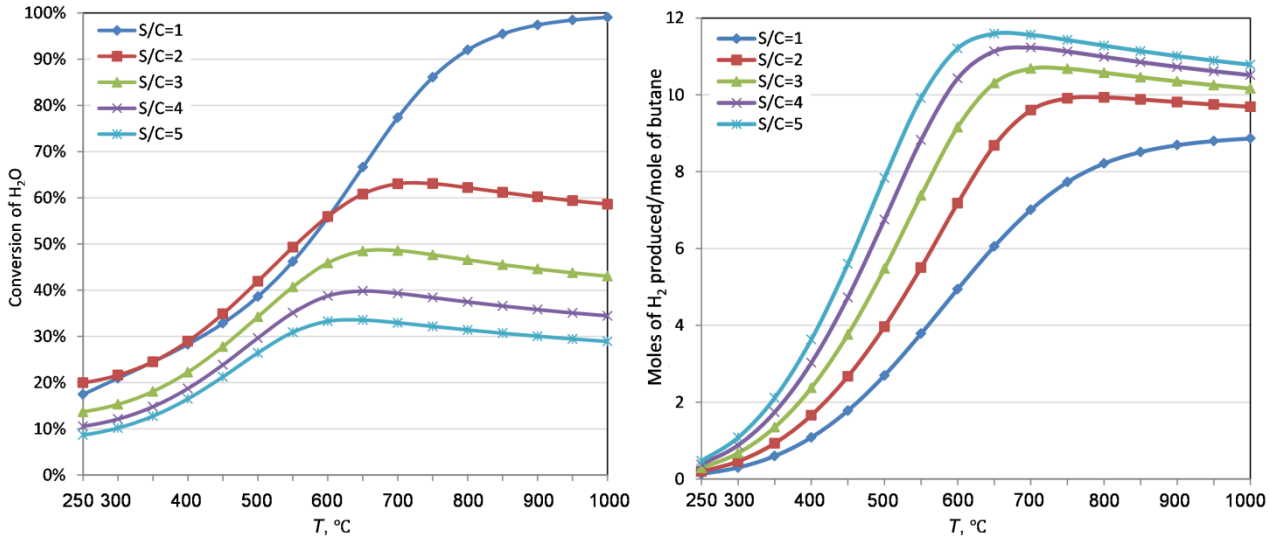

(a)

(b)

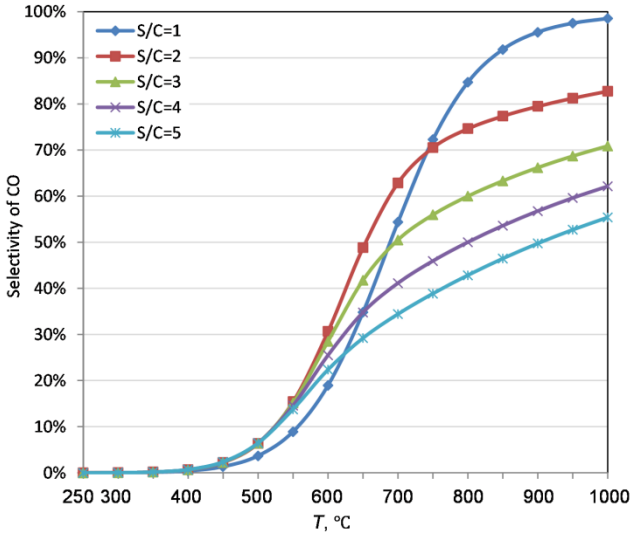

(c)

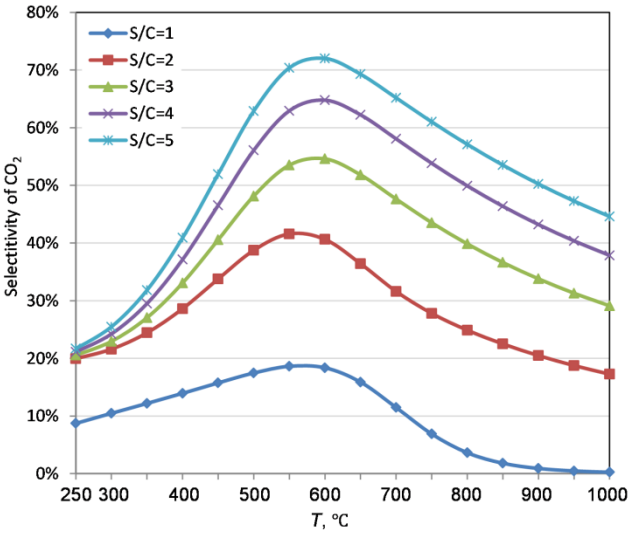

(d)

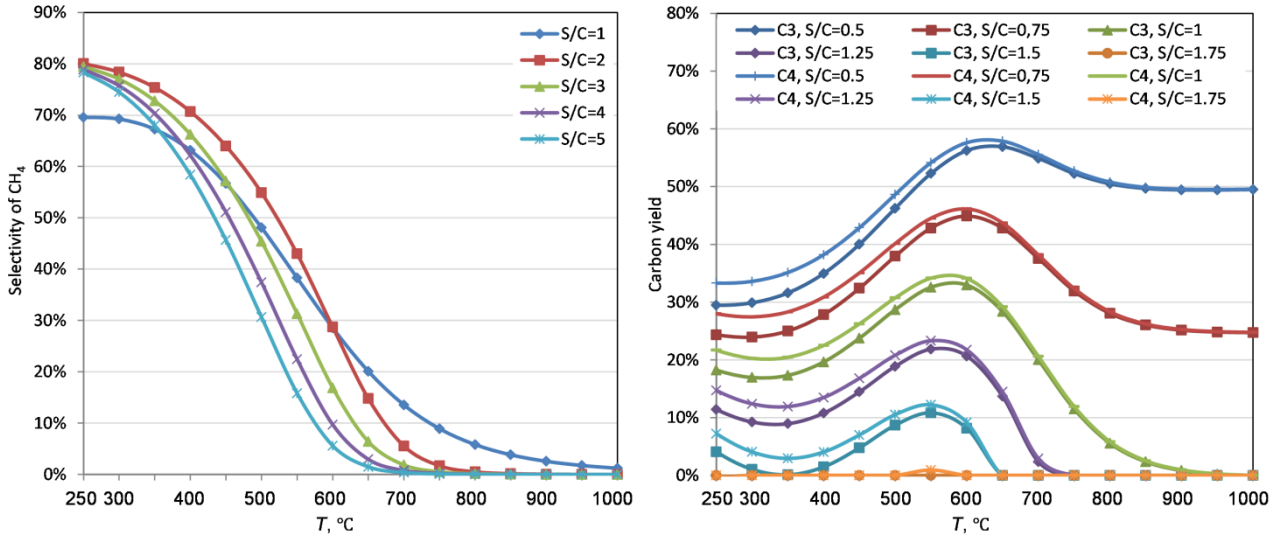

(e) (f)

Fig. 4. Equilibrium conversion of the reactants, selectivities and yield of the products for butane steam reforming as a function of temperature and S/C ratio at 1 atm.

3.2.3 Selectivities of CO, CO_2 and CH_4

Fig. 4(c) – (e) show the selectivity of CO, CO_2 and CH_4 in the products as a function of temperature and S/C ratio. Removal of CO in the product of BSR is usually necessary for fuel cell applications by subsequent WGS reactors. Therefore, the CO content in the product may influence the load and cost of the downstream WGS processes (e.g., the amount of catalyst required for WGS reactors). The CO selectivity increased with increasing temperature and decreased with increasing S/C ratio. The former trend is mainly ascribed to the promotion of the endothermic reforming process (reaction 1–9) and reverse WGS reaction (reaction 10) at higher temperatures, whereas for the latter trend the higher S/C ratios convert more CO to CO_2 by the WGS reaction (reaction 10) and result in lower levels of CO selectivity. The CO_2 selectivity (shown in Fig. 4(d)) was influenced by these two processes (reaction 1–10). With the increase of the temperature, maximum CO_2 selectivities at 550–600℃ can be found due to both the increase of CO and the suppression of the WGS reaction at high temperatures.

The methane in the products originates mainly from the cracking reactions of the heavy components (e.g., reaction 13, 16 and 18) as well as the methanation reactions (e.g., reverse reaction of reaction 1). As shown in Fig. 4(e), the produced methane was further converted with the increase of temperature through reaction 1 and 18. A low level of methane content in the product can be achieved at high

temperatures, e.g., CH_4 selectivity is less than 2% under the conditions of T > 650℃, S/C = 5, T > 700℃, S/C = 3 and 4, T > 750℃, S/C =2, and T > 950℃, S/C =1. Proper conditions aiming at limited CH_4 selectivity and lower CO selectivity can be chosen according to Fig. 4, e.g., the conditions of T = 650–750℃, S/C = 3 result in 41.8%–56.0% of CO, 43.5%–51.8% of CO_2 and 0.5–6.4% of CH_4 in the product.

Compared to the results of PSR, a lower CO_2 selectivity and higher CH_4 selectivity were found for BSR. However, the differences in the selectivity values between the results from PSR and those from BSR are very close (ΔS_{CO} < 0.2%, ΔS_{CO_2} < 2.0% and ΔS_{CH_4} < 3.8%). Due to the higher number of carbon atoms in butane, greater amounts of products were generated from each mole of butane than from propane, e.g., X_{CO} = 23.8–30.6%, X_{CO_2} = 25.3–32.6% and X_{CH_4} = 19.4–23.3% under the investigated conditions.

3.2.4 Carbon formation

Low S/C ratios may result in carbon formation on the catalyst through reactions 18–22. Fig. 4(f) presents the equilibrium carbon yields at different temperatures and S/C ratios (0.5–1.75) for both the PSR and BSR processes. BSR shows higher carbon yields than PSR especially at low and moderate temperatures (e.g., T < 650℃, S/C = 1), and the results for both of two processes are closer to each other with the increase of the temperature (e.g., T > 650℃, S/C = 1). Regarding the amounts of carbon formation per mole of hydrocarbon feed, BSR is more prone to carbon formation than PSR, e.g., the amount is more than 25.1% higher under all the investigated conditions (shown in Figure 2S in Appendix A). Maximum level of carbon formation were found for each S/C ratio at the moderate temperature range of 550–650℃, which is consistent with the simulation results for PSR [75] and the coke-promoting temperature range reported in the experimental study [6]. The decrease of carbon formation at high temperatures is due to the suppression of the exothermic reactions 18, 20–21, and the decrease of the CH_4 content in reaction 19. It should be noted that reaction 22 was not considered in the present thermodynamic analysis which could result in pyrolytic carbon encapsulating the catalyst at high temperatures (> 650℃) [18].

For higher S/C ratios, a thermodynamically carbon-free zone was found, e.g., S/C > 1.75 for PSR and S/C > 2 for BSR, which can be easily achieved by the typical S/C ratios (2.5–3) used in industry. For the designs using low S/C ratios, higher operating temperatures are required to avoid the carbon-promoting temperature range mentioned above (e.g., for S/C=1.5, T > 650 is needed). It is important to

note that carbon formation could also occur in the thermodynamically carbon-free zone in practical SR processes for different reasons, e.g., due to a poor distribution of gases in the local area of the reformer and a carbon formation rate that is greater than the rate of the carbon removal by the reactions on the catalyst surface.

3.3 Oxidative steam reforming of butane

Oxygen or air can be introduced into an SR process with the following aims: 1. Reducing the external heat supply of the reformer through the exothermic POX reactions of hydrocarbons (reaction 23–24); 2. Removal or decrease of the carbon deposition on the catalyst surface by carbon oxidation (e.g., reaction 26) and reduction of olefins in the gas phase as mentioned in section 3.1.2. It should be noted that limitations should also be considered for the OSR process, e.g., the additional cost of oxygen or air supply system, heat transfer consideration (e.g., hot point) for the reformer design with the fast exothermic POX reactions as well as the catalyst stability under oxidative atmosphere (e.g., the oxidation and deactivation of nickel-based catalysts [17]).

The equilibrium conversion of the reactants, selectivities of the products and the hydrogen produced for OSR of butane (1 mol/s) at different temperatures (250–1000°C), O_2/HC ratios (0.4–2.4) and the typical S/C ratio of 3 are shown in Fig. 5. Furthermore, the equilibrium yields of carbon at low S/C ratios (0.5 and 1.25) are shown in Fig. 6, whereas no carbon formation was found for higher investigated S/C ratios (i.e., S/C $\geq$ 1.75). The result of BSR with the same S/C ratio condition was also shown in Fig. 5 and Fig. 6 for comparison. The analysis of propane oxidative steam reforming (POSR) was also investigated for comparison (not shown in Figs. 5 and 6). The trends of butane oxidative steam reforming (BOSR) were found to be similar to those of POSR both in the present study and in the literature [20]. Butane and oxygen were completely converted under all investigated conditions.

3.3.1 Conversion of H_2O

The OSR process can be viewed as a combination of the POX and SR processes [17]. As mentioned in section 3.1.1, the POX reactions (reaction 23–24) have higher thermodynamic equilibrium constants and occur more easily than the SR reactions. Consequently, compared to BSR, the conversion of H_2O for BOSR decreased when O_2 was added in the feed as shown in Fig. 5(a), and the decrease of the H_2O conversion was almost linear with the increasing O_2/HC ratio. This conversion decrease also indicates that there will be more unconverted water in the system for BOSR compared to BSR, e.g., at 650°C and

S/C=3, the conversion of water is 48.5% for BSR, and 33.7% (O_2/HC=1.2) and 23.1% (O_2/HC=2.0) for BOSR. Compared to BOSR, the H_2O conversion values for POSR are slightly lower with the difference of ΔC_{H_2O} < 5% for the investigated S/C (1–5) and O_2/HC ratios (0.4–2.4).

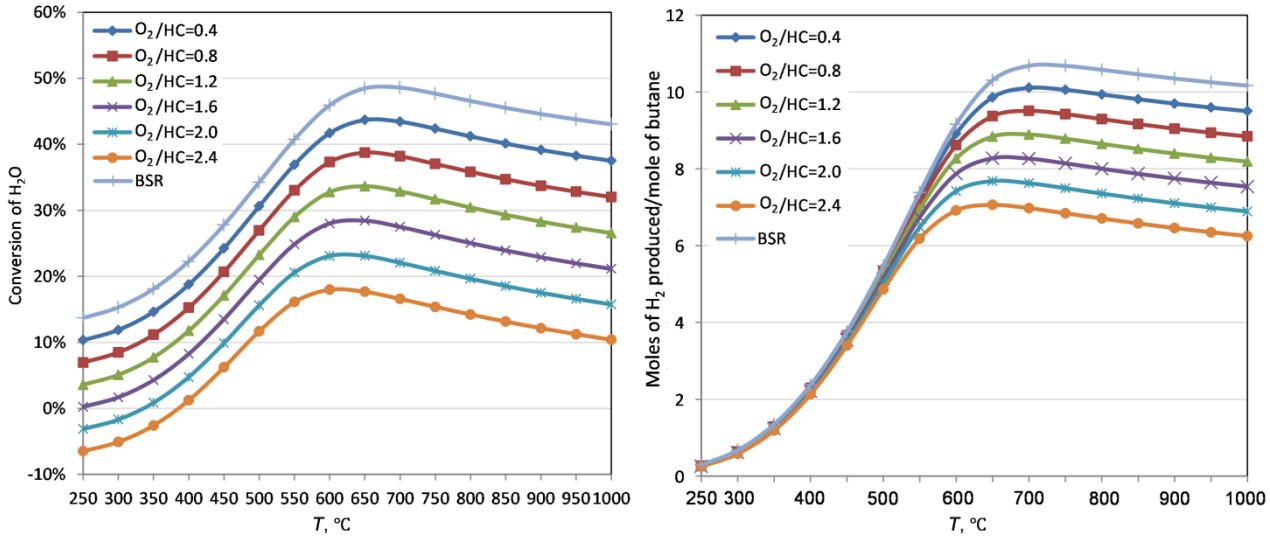

(a)

(b)

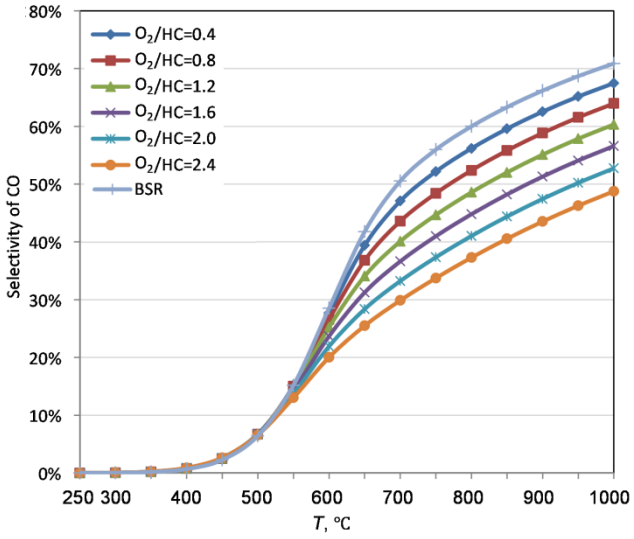

(c)

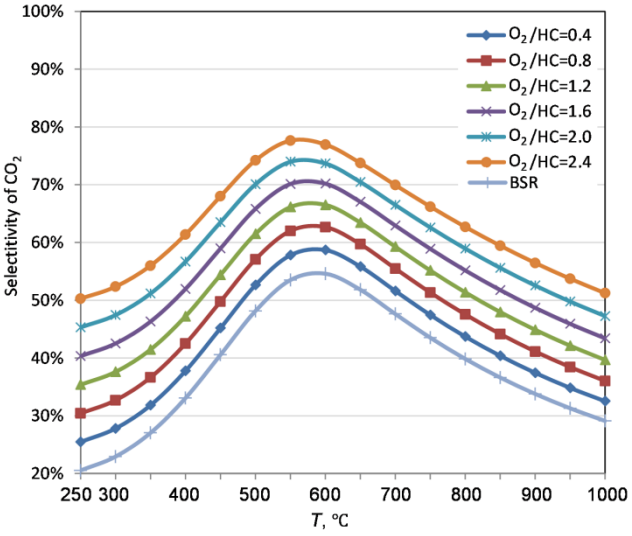

(d)

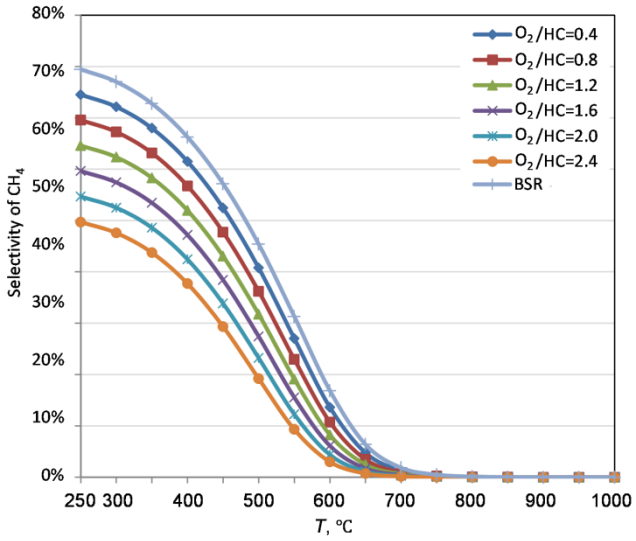

(e)

Fig. 5. Equilibrium conversion of the reactants, selectivities and yield of the products for BOSR as a function of temperature and O_2/HC ratio at 1 atm and S/C = 3.

3.3.2 H_2 yield

Compared to the SR reactions, the POX reactions (reaction 23–24) produce less hydrogen because O_2 is not a source of hydrogen. As shown in Fig. 5(b), for the BOSR process, the H_2 yields decreased with the rising O_2/HC ratio, which is more obvious at moderate and high temperatures. For instance, at 650℃ and S/C=3, the amount of H_2 produced is 10.3 mol/mol butane for BSR, 8.8 mol/mol butane (O_2/HC = 1.2) and 7.7 mol/mol butane (O_2/HC = 2.0) for BOSR.

Although the increasing O_2/HC ratio results in a lower H_2 yield according to the thermodynamic predictions, experimental results showed that the addition of a low level of O_2 can result in a positive effect on the H_2 yield [13][16]. Laosiripojana and Assabumrungrat [13] studied the autothermal reforming of LPG over a CeO_2 catalyst at 900℃ and found that the H_2 selectivity increased with increasing O/C molar ratio when O/C is less than 0.6. Silva et al. [16] conducted the OSR of LPG over $La_{1-x}Ce_xNiO_3$ and $La_{1-x}Sr_xNiO_3$ catalysts, and higher H_2 production was obtained at 873 K and O_2/LPG = 0.25 than under the SR conditions. The positive effects of O_2 in the above studies can be ascribed to the promotion of the removal of the carbon formed on the surface of the catalyst. For the OSR of propane, the H_2 produced from BOSR is 20.4–23.4% higher than that from POSR, which is similar to the results for the SR process (see section 3.2.2).

3.3.3 Selectivities of CO, CO_2 and CH_4

Figs. 5(c)–(e) demonstrate the selectivities of CO, CO_2 and CH_4 in the products as a function of temperature and O_2/HC ratio at S/C = 3. The CO selectivity decreased with increasing O_2/HC ratio as shown in Fig. 5(c), because in the presence of more the oxidant (O_2) in the system, more CO will be oxidized and converted to CO_2 through the WGS reaction (reaction 10) or reaction 25 (for the conditions with high O_2/HC ratios). Therefore, the CO_2 selectivity increased with the increasing O_2/HC ratio (see Fig. 5(d)). For example, at the typical temperature of 650℃, S/C=3 and O_2/HC = 1.2, the equilibrium selectivities of CO and CO_2 are 34.1% and 63.4%, respectively, whereas those for the SR condition are 41.8% and 51.8%, respectively. However, an experimental study showed that the CO molar fraction in the OSR condition can also be higher than that in the SR condition, because more CO may form through the oxidation of the coke deposition on the surface of catalyst [16].

Methane selectivity decreased with the increase of the O_2/HC ratio (see Fig. 5(e)), which could be ascribed to the lower content of CO and H_2 and a higher H_2O level in the system that can promote the conversion of CH_4 through the reforming reaction (reaction 1). In additions, a higher fraction of O_2 (for the conditions with high O_2/HC ratios) and CO_2 in the system can also oxidize CH_4 by reaction 23–24 and the dry reforming reaction (CO_2+CH_4↔2CO+2H_2). Compared with BSR, lower level of CH_4 selectivity can be obtained by BOSR, e.g., the CH_4 selectivity is less than 2% under the condition of T > 650℃, O_2/HC >1.2, whereas higher temperature range of T > 700℃ is needed for BSR to achieve the same CH_4 selectivity。

Compared to the results of POSR with the same O_2/C ratios (C represents moles of carbon atom in the feed), the differences in the selectivity values between the POSR and BOSR results are still quite small (ΔS_{CO} < 1.0%, ΔS_{CO_2} < 2.0% and ΔS_{CH_4}< 3.8%), similar to the results for the SR condition. The number of moles of the products generated from each mole of butane are higher than those from each mole of propane (X_{CO} = 22.6–29.4%, X_{CO_2} = 25.5–31.1% and X_{CH_4} = 14.6–23.1%) under the investigated conditions (T = 250–1000℃, O/C = 0.2–1.2 and S/C = 1–5).

3.3.4 Carbon formation

Fig. 6 shows the equilibrium carbon yields of OSR of butane (1 mol/s) at different temperatures, S/C ratios (0.5 and 1.25) and O_2/HC ratios. The carbon yield decreased with the increasing S/C ratios and O_2/HC ratios. Compared to the SR condition, the carbon-free zones were further enlarged with the increasing O_2/HC ratios. Especially, at the low S/C ratios of 0.5 shown in Fig. 6(a), carbon formation

was always observed at the investigated temperatures under the SR conditions, whereas under the OSR condition, carbon-free zone can be achieved by using appropriate O_2/HC ratios, e.g., O_2/HC > 1.2 for S/C = 0.5. The carbon-free zones were also enlarged with a higher S/C ratio as shown in Fig. 6(b), which is similar to the trend under the SR condition. In addition, the carbon yields of BOSR with other S/C ratios can be found in Fig 3S in Appendix A.

Regardless of the oxidation of the formed carbon by reaction 26, the olefins (could form by the cracking reactions mentioned in section 3.1.2) in the system can also be oxidized and decreased to lower level by O_2 as mentioned for the POX process (in section 3.1.2); for example, an experimental study of the autothermal reforming of LPG [13] showed that there was no ethylene detected in the products under the conditions of O/C ≥ 0.6, S/C = 1.45 and 900℃. Consequently, the carbon formation through reaction 18 and reaction 22 can also be lower or removed by using a proper O_2/HC ratio.

The carbon yields for the OSR of propane and butane with the same O_2/C ratios are close ($Y_{carbon,\ butane} - Y_{carbon,\ propane} < 5\%$) especially at high temperatures, which is similar to the trends for the SR conditions (see Fig. 4(f)). For the moles of carbon formation per mole of hydrocarbon feed, the carbon formation per mole of butane is more than 24.5% higher than the corresponding values for POSR under the same investigated conditions.

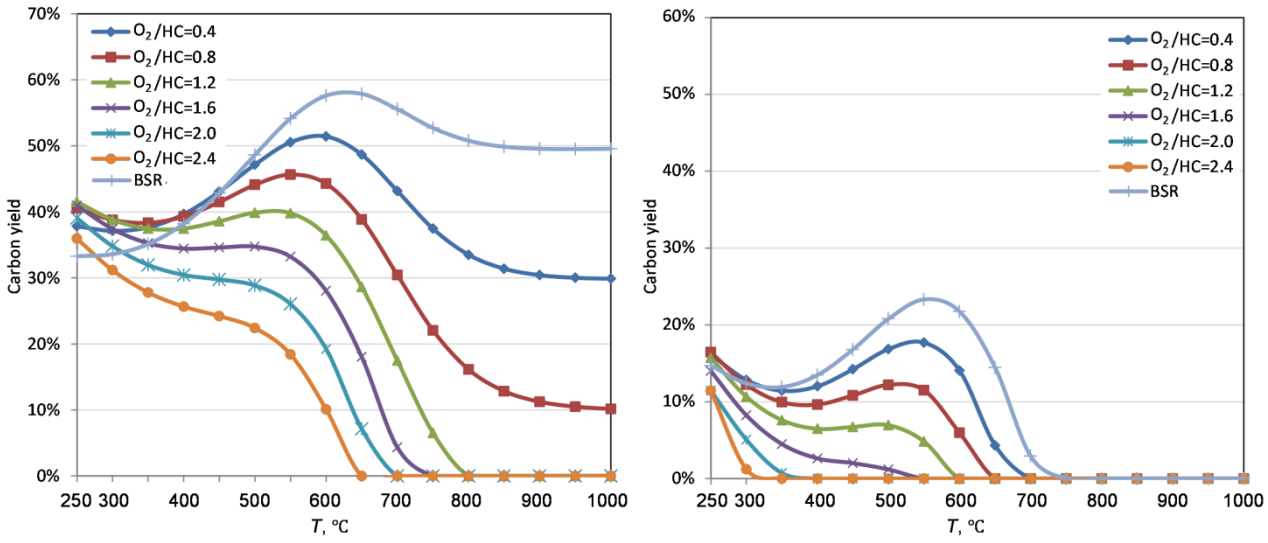

(a) (b)

Fig. 6. Equilibrium carbon yield for BOSR as a function of temperature and O_2/HC ratio at 1 atm and different S/C ratios: (a) S/C = 0.5; (b) S/C = 1.25.

3.3.5 Thermo-neutral conditions

For an oxidative steam reforming process, thermo-neutral (TN) conditions can be achieved with proper O_2/HC ratio in the feed, where the total reaction enthalpy of the endothermic SR reactions, the exothermic POX and WGS reactions and other reactions in the system approach zero, and no external heat supply is needed. This operation is also called the autothermal reforming (ATR). Fig. 7 illustrates the TN temperatures for ATR of propane and butane at different O/C (oxygen atom in H_2O was not included in this molar ratio) and S/C ratios in the feed. The TN temperature increases with the increasing O/C ratios (0.1–0.6). TN conditions cannot be achieved when the O/C ratio is higher than 0.7 for both the ATR of propane and butane, which is close to the O/C ratio (approximately 0.72) predicted by Daniel and Dushyant [33] for ATR of different hydrocarbon fuels. However, an O/C ratio higher than 0.7 can be used for a practical system (e.g., O/C = 0.74–1.33 in [5]), where other heat requirements (e.g., heat loss to environment) in the reforming system are needed to be covered from the exothermic POX reactions.

Due to the promotion of the endothermic SR reactions by higher S/C ratios, the TN temperatures decrease with the increase of the S/C ratio for most conditions in Fig. 7. The trend is different for the conditions of O/C = 0.6 for ATR of butane where the exothermic WGS reaction may have larger influence while the high extent of the SR reactions has been achieved. The TN temperature differences between the ATR of butane and propane are within 8.6℃ for most conditions (except O/C = 0.6). The TN temperatures are below 750℃ under all investigated conditions. Carbon formation could occur for some of the TN conditions with lower S/C ratios, e.g., S/C = 0.5 which is not in the carbon-free zone mentioned in section 3.3.4.

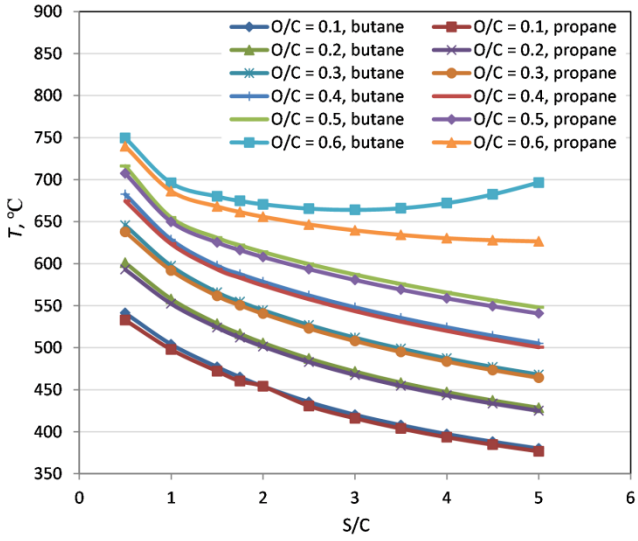

Fig. 7. Thermo-neutral temperatures for ATR of propane and butane as a function of O/C and S/C ratio.

4. Conclusions

The thermodynamic analyses of cracking, POX, SR and OSR of butane and propane (for comparison) were performed using the Gibbs free energy minimization method under the conditions of T = 250–1000°C, S/C = 0.5–5 and O_2/HC = 0–2.4. The simulations for the cracking of butane and propane showed that olefins (C_2–C_4) and acetylene (at high temperatures) can be easily generated and could also exist in an LPG steam reformer and increase the risk of carbon formation on the catalysts. The results from POX of butane demonstrated that most of the olefins and acetylene in the system can be oxidized and removed by adding an appropriate amount of oxygen, e.g., the level of olefins and acetylene is lower than 2% when O_2/HC ≥ 1.2.

For the SR process, maximum values of H_2O conversion and H_2 yield were found at 600–750°C for S/C = 2–5, and the values decreased slightly at higher temperatures, whereas monotonic trends were found with S/C = 1. Low CH_4 selectivity can be achieved only at high temperatures. The CO selectivity obviously increased with the increasing temperature at moderate and high temperatures (T > 500°C) which may influence the CO content in the products and downstream WGS reactors. Predicted carbon formation only occurred at low S/C ratios for BSR (S/C ≤ 2) and PSR (S/C ≤ 1.75), while the maximum level of carbon formation was found at 550–650°C.

Similar trends with temperature and S/C ratio were found for the OSR process, the results (except carbon formation) were almost linearly influenced by the O_2/HC ratio values. The addition of oxygen decreased the H_2O conversion, H_2 yield, selectivity of CO and CH_4 and increased the CO_2 selectivity. Especially, the carbon formation can be further removed compared to the SR conditions which results in larger carbon-free zones at low S/C ratios. For ATR operation of butane and propane, the TN temperatures decrease with the increase of the S/C ratio (except for O/C = 0.6) and the decrease of the O/C ratio. The TN temperatures are below 750°C under all investigated conditions. The simulated results (conversion, selectivity) for SR or OSR of propane and butane are very close (ΔC_i or ΔS_i < 5%) under the investigated conditions; one mole of butane produces approximately 15%–33% higher moles of products (H_2, CO, CO_2, CH_4 and carbon) than propane.

Acknowledgement

The authors would like to acknowledge the support of this work from the Danish Energy Agency (EUDP, 64011-0025) funded project USDan and the collaboration with Ballard Europe.

References

[1] Joensen F, Rostrup-Nielsen JR. Conversion of hydrocarbons and alcohols for fuel cells. J Power Sources 2002; 105: 195–201.

[2] Song CS. Fuel processing for low-temperature and high-temperature fuel cells: Challenges, and opportunities for sustainable development in the 21st century. Catal Today 2002; 77: 17–49.

[3] Morganti KJ, Foong TM, Brear MJ, Silva GD, Yang Y, Dryer FL. The Research and Motor octane numbers of Liquefied Petroleum Gas (LPG). Fuel 2013; 108: 797–811.

[4] Silberova B, Venvik HJ, Holmen A. Production of hydrogen by short contact time partial oxidation and oxidative steam reforming of propane. Catal Today 2005; 99: 69–76.

[5] Çağlayan BS, Avcı AK, Önsan ZI, Aksoylu AE. Production of hydrogen over bimetallic Pt–Ni/δ-Al_2O_3 I. Indirect partial oxidation of propane. Appl Catal A Gen 2005; 280: 181–188.

[6] Schädel BT, Duisberg M, Deutschmann O. Steam reforming of methane, ethane, propane, butane, and natural gas over a rhodium-based catalyst. Catal Today 2009; 142: 42-51.

[7] Modafferi V, Panzera G, Baglio V, Frusteri F, Antonucci PL. Propane reforming on Ni–Ru/GDC catalyst: H_2 production for IT-SOFCs under SR and ATR conditions. Appl Catal A Gen 2008; 334: 1–9.

[8] Jo SW, Im YH, Do JY, Park NK, Lee TJ, Lee ST, Cha MS, Jeon MK, Kang M. Synergies between Ni, Co, and Mn ions in trimetallic $Ni_{1-x}Co_xMnO_4$ catalysts for effective hydrogen production from propane steam reforming. Renewable Energy 2017; 113: 248–256.

[9] Sato K, Sago F, Nagaoka K, Takita Y. Preparation and characterization of active Ni/MgO in oxidative steam reforming of n-C_4H_{10}. Int J Hydrogen Energy 2010; 35: 5393–5399.

[10] Jeong H, Kang M. Hydrogen production from butane steam reforming over Ni/Ag loaded $MgAl_2O_4$ catalyst. Appl Catal B Environ 2010; 95: 446–455.

[11] Park K, Lee SH, Bae GJ, Bae JM. Performance analysis of Cu, Sn and Rh impregnated NiO/CGO91 anode for butane internal reforming SOFC at intermediate temperature. Renewable Energy 2015; 83: 483–490.

[12] Gökaliler F, Çağlayan BS, Önsan ZI, Aksoylu AE. Hydrogen production by autothermal reforming of LPG for PEM fuel cell applications. Int J Hydrogen Energy 2008; 33: 1383–1391.

[13] Laosiripojana N, Assabumrungrat S. Hydrogen production from steam and autothermal reforming of LPG over high surface area ceria. J Power Sources 2006; 158: 1348–1357.

[14] Laosiripojana N, Sutthisripok W, Kim-Lohsoontorn P, Assabumrungrat S. Reactivity of Ce-ZrO_2 (doped with La-, Gd-, Nb-, and Sm-) toward partial oxidation of liquefied petroleum gas: Its application for sequential partial oxidation/steam reforming. Int J Hydrogen Energy 2010; 35: 6747–6756.

[15] Zou XJ, Wang XG, Li L, Shen K, Lu XG, Ding WZ. Development of highly effective supported nickel catalysts for pre-reforming of liquefied petroleum gas under low steam to carbon molar ratios. Int J Hydrogen Energy 2010; 35: 12191–12200.

[16] Silva PP, Ferreira RAR, Noronha FB, Hori CE. Hydrogen production from steam and oxidative steam reforming of liquefied petroleum gas over cerium and strontium doped $LaNiO_3$ catalysts. Catal Today 2017; 289: 211–221.

[17] Malaibari ZO, Amin A, Croiset E, Epling W. Performance characteristics of Mo–Ni/Al_2O_3 catalysts in LPG oxidative steam reforming for hydrogen production. Int J Hydrogen Energy 2014; 39: 10061–10073.

[18] Rostrup-Nielsen JR. Production of synthesis gas. Catal Today 1993; 18: 305–324.

[19] Ahmed S, Krumpelt M. Hydrogen from hydrocarbon fuels for fuel cells. Int J Hydrogen Energy 2001; 26: 291–301.

[20] Zeng GM, Tian Y, Li YD. Thermodynamic analysis of hydrogen production for fuel cell via oxidative steam reforming of propane. Int J Hydrogen Energy 2010; 35: 6726–37.

[21] Wang X, Wang N, Zhao J, Wang L. Thermodynamic analysis of propane dry and steam reforming for synthesis gas or hydrogen production. Int J Hydrogen Energy 2010; 35: 12800–7.

[22] Nikoo MK, Amin NAS. Thermodynamic analysis of carbon dioxide reforming of methane in view of solid carbon formation. Fuel Process Technol 2011; 92: 678–691.

[23] Soria MA, Mateos-Pedreroa C, Guerrero-Ruiz A, Rodríguez-Ramos I. Thermodynamic and experimental study of combined dry and steam reforming of methane on Ru/ ZrO_2-La_2O_3 catalyst at low temperature. Int J Hydrogen Energy 2011; 36: 15212–15220.

[24] Giehr A, Maier L, Schunk SA, Deutschmann O. Thermodynamic considerations on the oxidation state of Co/γ-Al_2O_3 and Ni/γ-Al_2O_3 catalysts under dry and steam reforming conditions. ChemCatChem 2018; 10: 751–757.

[25] Großmann K, Dellermann T, Dillig M, Karl J. Coking behavior of nickel and a rhodium based catalyst used in steam reforming for power-to-gas applications. Int J Hydrogen Energy 2017; 42: 11150–11158.

[26] Silva PP, Ferreira RA, Nunes JF, Sousa JA, Romanielo LL, Noronha FB, Hori CE. Production of hydrogen from the steam and oxidative reforming of LPG Thermodynamic and experimental study. Braz J Chem Eng 2015; 32: 647–662.

[27] Wang JH, Chen H, Tian Y, Yao MF, Li YD. Thermodynamic analysis of hydrogen production for fuel cells from oxidative steam reforming of methanol. Fuel 2012; 97: 805–811.

[28] Nahar GA, Madhani SS. Thermodynamics of hydrogen production by the steam reforming of butanol: Analysis of inorganic gases and light hydrocarbons. Int J Hydrogen Energy 2010; 35: 98–109.

[29] Ness HCV, Abbott MM. Thermodynamics. In: R.H. Perry, D.W. Green. Perry's Chemical Engineers' Handbook, eighth ed. New York: McGraw-Hill; 2008. p. 4-28.

[30] Alvarado FD, Gracia F. Steam reforming of ethanol for hydrogen production: thermodynamic analysis including different carbon deposits representation. Chem Eng J 2010; 165: 649–657.

[31] Ghenciu AF. Review of fuel processing catalysts for hydrogen production in PEM fuel cell systems. Curr Opin Solid State Mater Sci 2002; 6: 389–399.

[32] Rostrup-Nielsen J, Christiansen LJ. Concepts in syngas manufacture. London: Imperial College Press; 2011.

[33] Haynes DJ, Shekhawat D. Oxidative Steam Reforming. In: Shekhawat D, Spivey JJ, Berry DA, editors. Fuel Cells: Technologies for Fuel Processing. Amsterdam: Elsevier Science; 2011. p. 137.

Appendix A

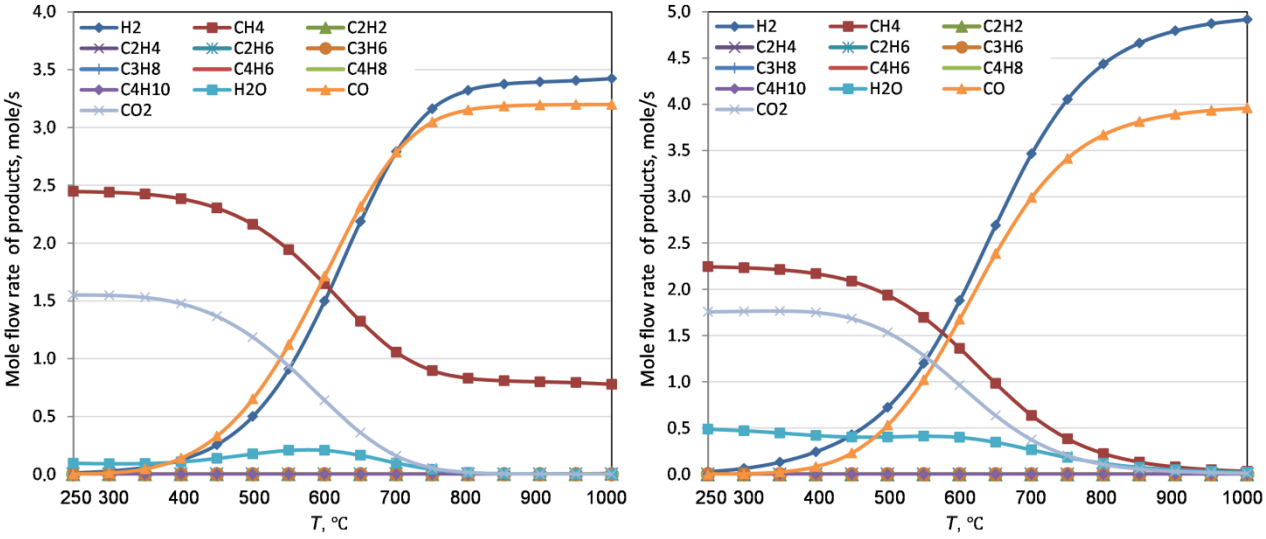

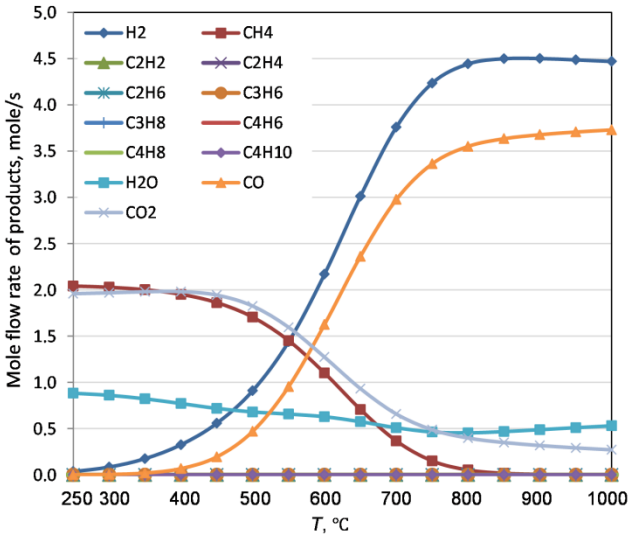

Figure 1S . Mole flow rates of the products of POX of butane (1 mol/s) as a function of temperature and O_2/C_4H_{10} ratio at 1 atm (a) $O_2/C_4H_{10} = 1.6$; (b) $O_2/C_4H_{10} = 2.0$; (c) $O_2/C_4H_{10} = 2.4$.

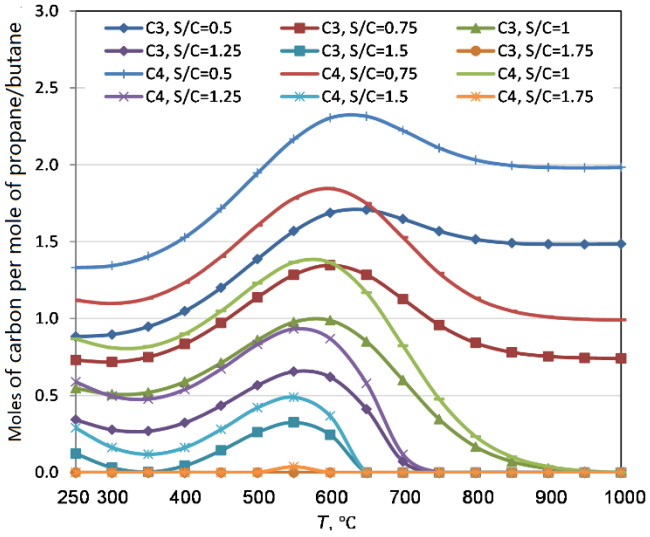

Figure 2S. Equilibrium carbon formation (in mole numbers) for BSR and PSR as a function of temperature and different S/C ratios.

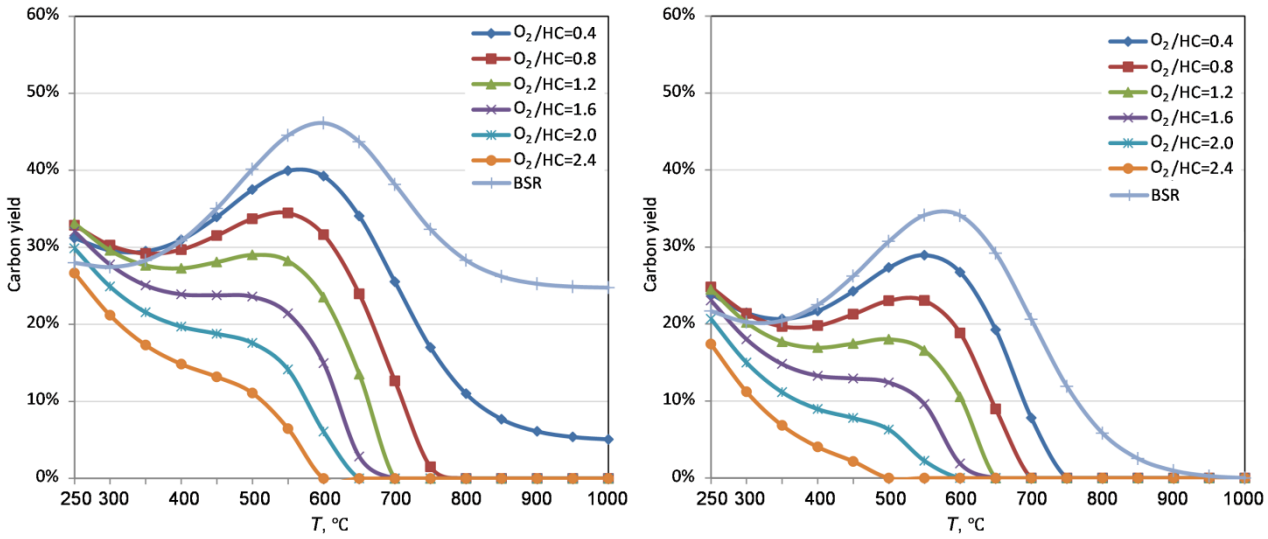

(a) (b)

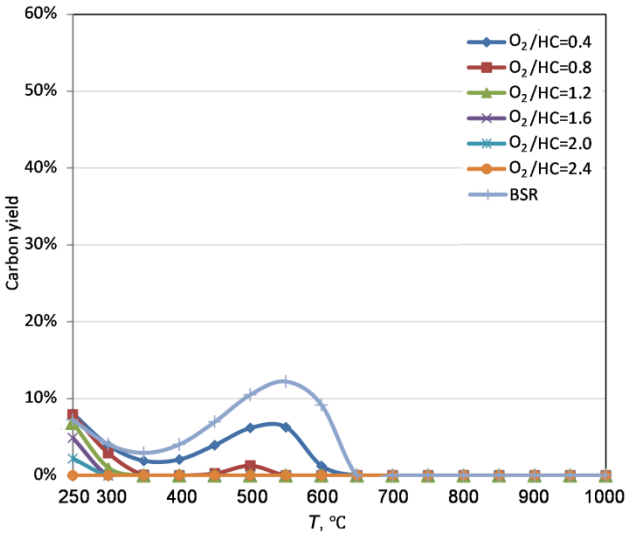

(c)

Figure 3S. Equilibrium carbon yield for BOSR as a function of temperature and O_2/HC ratio at 1 atm and different S/C ratios: (a) S/C = 0.75; (b) S/C = 1.00; (c) S/C = 1.5.